Available online at www.sciencedirect.com
SCIENCE DIRECT
International Journal of Pharmaceutics 315 (2006) 110–121
INTERNATIONAL JOURNAL OF PHARMACEUTICS
www.elsevier.com/locate/ijpharm

Controlled release of a self-emulsifying formulation from a tablet dosage form: Stability assessment and optimization of some processing parameters

Sami Nazzal [a,*], Mansoor A. Khan [b]

[a] *Department of Basic Pharmaceutical Sciences, College of Pharmacy, University of Louisiana at Monroe, Monroe, LA, USA*
[b] *Division of Product Quality Research, Food and Drug Administration, Federal Research Center, Silver Spring, MD, USA*

Received 23 November 2005; received in revised form 12 February 2006; accepted 13 February 2006
Available online 6 March 2006

Abstract

The objective of this study was to evaluate the effect of some processing parameters on the release of lipid formulation from a tablet dosage form. A 17-run, face-centered cubic design was employed to evaluate the effect of colloidal silicates (X_1), magnesium stearate mixing time (X_2), and compression force (X_3) on flow, hardness, and dissolution of Coenzyme Q_{10} (CoQ_{10}) lipid formulation from a tablet dosage form. The optimized formulation was subsequently subjected to a short-term accelerated stability study. All preparations had a flowability index values ranging from 77 to 90. The cumulative percent of CoQ_{10} released within 8 h (Y_5) ranged from 40.6% to 90% and was expressed by the following polynomial equation: $Y_5 = 49.78 - 16.36X_1 + 2.90X_2 - 3.11X_3 - 0.37X_1X_2 + 1.06X_1X_3 - 1.02X_2X_3 + 11.98X_1^2 + 10.63X_2^2 - 7.10X_3^2$. When stored at 4 °C, dissolution rates were retained for up to 3 months. Storage at higher temperatures, however, accelerated lipid release and caused leakage, and loss of hardness. Processing parameters have a profound effect on the release of lipid formulations from their solid carriers. While optimized controlled release formulations could be attained, further considerations should be made to prepare "liquisolids" that are physically stable at higher storage temperatures.

Keywords: Self-emulsified drug delivery system; Coenzyme Q_{10}; Optimization; Controlled release; Face-centered cubic design; Stability

1. Introduction

Large proportions of new drug candidates have poor water solubility. To overcome this barrier many formulation strategies, such as complexation with cyclodextrins, solid dispersions and co-precipitates were developed and reported in the literature (Perng et al., 1998; Nazzal et al., 2002a). In recent years, however, much attention has been focused on lipid-based formulations with particular emphasis on self-emulsifying drug delivery systems (Pouton, 2000). Self-emulsifying drug delivery systems (SEDDS) are isotropic mixtures of oil, surfactant, co-surfactant and drug that form fine oil-in-water emulsion when introduced into aqueous medium under gentle agitation (Charman et al., 1992; Craig et al., 1993; Gao et al., 1998). Recently, a novel eutectic-based self-nanoemulsified drug delivery system (SNEDDS) of ubiquinone was introduced (Nazzal and Khan, 2002; Nazzal et al., 2002c). This lipid formulation was subsequently incorporated into a tablet dosage form, which was termed "liquisolid" or solid-lipid compact, using blends of maltodextrin, modified povidone, and micro crystalline cellulose (MCC) (Nazzal et al., 2002b,d).

Incorporation of a lipid formulation into a solid dosage form combines the advantages of a lipid-based drug delivery system with those of a solid dosage form, and overcomes some of the shortcomings of liquid formulations (Cannon, 2005). Formulating liquid medications into solid compacts has been the interest of many studies. Jarowski (Yang et al., 1979; Liao and Jarowski, 1984) and later Spireas (Spireas et al., 1992; Spireas and Sadu, 1998) worked on producing solid solutions and "liquisolids" based on the concept of blending liquid medications with selected powder excipients to produce free flowing, readily compressible powders. Later, pellets containing a self-emulsifying

* Corresponding author at: Department of Basic Pharmaceutical Sciences, College of Pharmacy, University of Louisiana at Monroe, 700 University Avenue, Monroe, LA 71209-0497, USA. Tel.: +1 318 342 1726; fax: +1 318 342 1737.
E-mail address: nazzal@ulm.edu (S. Nazzal).

0378-5173/$ – see front matter © 2006 Elsevier B.V. All rights reserved.
doi:10.1016/j.ijpharm.2006.02.019

mixture were prepared by extrusion/spheronization (Newton et al., 2001); a solid-state microemulsion for the delivery of cyclosporine was prepared by coating a pre-microemulsion with an enteric coating material (Kim et al., 2001). Similarly, solvent evaporation method was used to prepare tocopheryl nicotinate tablets utilizing calcium silicates as the adsorbing agent (Takashima et al., 1999). A review of oral solid dosage forms of lipid-based drug delivery systems and the approaches undertaken to incorporate lipids into solid matrices was recently published in the American Pharmaceutical Review (Cannon, 2005) and the STP Pharma Pratiques (Jannin and Chambin, 2005).

"Liquisolids", or solid dosage forms of lipid formulations, which were reported in the literature, however, typically describe immediate release dosage forms. There are no documented controlled release "liquisolid" compacts that could release the lipid formulation from its solid carrier in a controlled release pattern over an extended period of time. Only few alternative technologies were reported that combine the features of controlled release and lipid-based formulations. A notable example is the L-Oros® Softcap™ delivery system, which was developed by Alza Corporation. This technology is based on coating liquid filled capsules with an osmotic layer and a rate controlling membrane (Dong et al., 2002). From a manufacturing perspective, however, it is more practical and economical to prepare tablets from directly compressible powder blends that could deliver the adsorbed lipid formulation in a controlled release pattern.

In a previous study (Nazzal et al., 2002d) we observed that the release of lipid formulations from a tablet dosage form could be controlled by the addition of microcrystalline cellulose of finer particle size (Avicel® PH-105, 20 μm). It is well established that the initial size of the particles constituting a powder is an important factor in determining its compaction behavior (Alderborn and Nystrom, 1982; Duberg and Nystrom, 1986). For most powdered materials, compaction of the smaller particles result in stronger tablets because of their larger surface area available for bonding (Sun and Grant, 2001). Fine processing adjuvants – such as colloidal silicates and magnesium stearate, which are commonly added as glidant and lubricating agents, respectively – and magnesium stearate mixing time were shown to have a profound effect on dissolution and drug release rate from conventional tablet dosage forms (Abdallah et al., 1983; Khan et al., 1983; Morasso et al., 1988; Wang and Chowhan, 1990). Among processing parameters, compaction force was also shown to have an effect on the dissolution rate, hardness and friability of different products (Dabbagh et al., 1996; Hariharan et al., 1997).

The effect of these processing parameters on the release of lipid formulations form its solid carrier is not reported in the literature. The objectives of the present study were therefore: (1) to demonstrate the effect of colloidal silicon dioxide (X_1), magnesium stearate mixing time (X_2), and compression force (X_3) on the physical properties and release rate of a CoQ_{10} lipid formulation from a tablet dosage form. The effect of these three processing parameters was evaluated by observing the release of CoQ_{10} lipid formulations from a powder blend, which was previously optimized by Nazzal et al. (2002b) to release 100% of CoQ_{10} within 45 min; (2) to optimize the level of these process parameters using a three-factor, three-level, face-centered cubic design; and (3) to evaluate the short-term stability of the optimized formulation after storage at accelerated stability conditions.

2. Materials and methods

2.1. Experimental design

A three-factor, three-level, face-centered cubic design was used in this study to construct a second order polynomial model for the optimization process. The design is a three-level fractional-factorial experiment suitable for exploring quadratic response surfaces. This design provides an empirical mathematical model to describe the effect of process variables on the product characteristics. The model is of the form: $Y = A_0 + A_1X_1 + A_2X_2 + A_3X_3 + A_4X_1X_2 + A_5X_2X_3 + A_6X_1X_3 + A_7X_1^2 + A_8X_2^2 + A_9X_3^2 + E$, where A_0–A_9 are the coefficients of the respective variables and their interaction terms, and E is an error term (Murray, 1994). The factors selected were amount of colloidal silicon dioxide (X_1), magnesium stearate mixing time (X_2), and compression force (X_3). An orthogonal design was used such that the factor levels were evenly spaced and coded for low, medium and high settings as −1, 0 and 1, respectively. Table 1 summarizes the dependent and independent variables evaluated and the constraints that were placed on the responses.

2.2. Materials

CoQ_{10} was a generous gift from Kyowa Hakko USA (New York, NY). Polyoxyl 35 castor oil (Cremophor® EL) and

Table 1
Variables in the face-centered cubic design

Independent variables	Levels		
	Low, −1	Middle, 0	High, 1
X_1 = amount of colloidal silicon dioxide (%)	1	3	5
X_2 = magnesium stearate mixing time (min)	2	4	6
X_3 = compression force (kg)	500	1250	2000
Dependent variables	**Constraints**		
	Low	High	Goal
Y_1 = cumulative percent of CoQ_{10} released in 1 h	7.5	17.5	12.5
Y_2 = cumulative percent of CoQ_{10} released in 2 h	20	30	25
Y_3 = cumulative percent of CoQ_{10} released in 4 h	45	55	40
Y_4 = cumulative percent of CoQ_{10} released in 6 h	70	80	75
Y_5 = cumulative percent of CoQ_{10} released in 8 h			Maximize
Y_6 = hardness (kg)	3	5	Maximize
Y_7 = flowability index (Carr's flow index)	N/A		
Y_8 = friability (%)	N/A		

copolyvidone (Kollidon® VA 64) were obtained from BASF Corp. (Mount Olive, NJ). Medium chain mono- and diglycerides (Capmul® MCM-C8) was obtained from Abitec Corp. (Janesville, WI). Single fold lemon oil type C.P. Extra FCC was obtained from Citrus and Allied essences Ltd. (Floral Park, NY). Maltodextrin with a mean particle diameter of 190 μm and a dextrose equivalent of 12.5 (Glucidex® IT 12) was obtained from Roquette America, Inc. (Keokuk, IA). Microcrystalline cellulose (Avicel® 1 PH-112) was obtained from FMC Corp. (Newark, DE). Magnesium stearate, NF-FCC was a gift from Whittaker, Clark, and Daniels Inc. (South Plainfield, NJ). Amorphous fumed silica (CAB-O-SIL® M-5P) was obtained form Cabot Corp. (Tuscola, IL). HPLC grade methanol and *n*-hexane were purchased from VWR Scientific (Minneapolis, MN). All the chemicals were used as received.

2.3. Preparation of the solid-lipid (liquisolid) powder blends

The eutectic-based self-nanoemulsified drug delivery system (SNEDDS) of CoQ_{10} was prepared as follows. CoQ_{10} and lemon oil at a ratio of 1:1 were accurately weighed into screw-capped glass vial and melted in water bath at 37 °C. Cremophor EL and Capmul MCM-C8 were added to the oily mix at a final concentration of 26.9% (w/w) each. The resultant emulsion was mixed with a stirring bar until a transparent solution of SNEDDS was obtained. The SNEDDS were then allowed to cool at ambient temperature for 24 h until a viscous paste was obtained. Detailed characterization of the eutectic-based drug delivery system can be found elsewhere (Nazzal et al., 2002c).

A powder blend was obtained by granulating the lipid (SNEDDS) paste with Kollidon VA 64, Glucidex IT 12, and Avicel PH-112. The amount of microcrystalline cellulose (Avicel PH-112), copolyvidone (Kollidon VA 64), and maltodextrin (Glucidex IT 12) used to prepare each tablet were 100, 66.6, 560.1 mg, respectively. Initially, the SNEDDS paste was mixed with copolyvidone using a high shear blender (Hamilton Beach) for 2 min. Maltodextrin was then added and the mixture was blended for 5 min to obtain uniformly sized granules. SNEDDS granules were then mixed with microcrystalline cellulose (MCC) in a V-blender for 5 min. MCC is critical to improve the hardness of the tablets. A V-blender was therefore used instead of the high shear mixer to prevent the incorporation of MCC into the granules. Silicon dioxide was blended with the mixture using a planetary mixer (Kenwood) at setting 4 for 3 min. Before compression, magnesium stearate was added to the granular mixture and mixed using the V-blender for the time specified in the experimental design (Table 1). In order to increase the hardness of the compacts without modifying the dissolution profile of the tablets, a second layer (backing support) made of 150 mg of Avicel® MCC PH-112 mixed with 1% magnesium stearate was added and compressed to make a double layered tablet dosage form. The amount of silicone dioxide (X_1), magnesium stearate mixing time (X_2), and compression force (X_3) used to prepare each of the 17 formulations are given in Table 2.

Table 2
Amount of silicon dioxide (X_1), magnesium stearate mixing time (X_2), and compression force (X_3), used in each of the 17 formulations of the face-centered cubic design

Run	X_1	X_2	X_3
1	−1	−1	−1
2	1	−1	−1
3	−1	1	−1
4	1	1	−1
5	−1	−1	1
6	1	−1	1
7	−1	1	1
8	1	1	1
9	−1	0	0
10	1	0	0
11	0	−1	0
12	0	1	0
13	0	0	−1
14	0	0	1
15	0	0	0
16	0	0	0
17	0	0	0

2.4. Carr's flowability index

The flow properties of the powdered lipid formulations were determined by the Carr's method. The following four tests were measured: (1) compressibility, (2) angle of repose, (3) angle of spatula, and (4) uniformity coefficient or cohesion. The flowability index (FI) was then calculated with the point scores as described (Carr, 1965).

2.4.1. Compressibility

The granular powder (10 g) was poured lightly into a 25 ml graduated cylinder. The powder was tapped until no further change in volume was observed. Powder bulk density, ρ_b (g/cm^3), and powder tapped density, ρ_p (g/cm^3) were calculated as the weight of the powder divided by its volume before and after tapping, respectively. Percentage compressibility was computed from the following equation:

$$\%\ \text{compressibility} = 100 \times \frac{\rho_p - \rho_b}{\rho_p}$$

2.4.2. Angle of repose

Angle of repose was measured using a protractor for the heap of granules formed by passing 10 g of the sample through a funnel at a height of 8 cm from the horizontal surface.

2.4.3. Angle of spatula

Angle of spatula was measured using a protractor and a steel spatula with a 5 in. × 7/8 in. blade. The spatula was inserted to the bottom of the heap that was carefully built by dropping the material through a funnel at a height of 8 cm from the horizontal surface. The spatula was then withdrawn vertically and the angle of the heap formed on the spatula was measured as the angle of spatula.

2.4.4. Uniformity coefficient

Uniformity coefficient was obtained by sieve analysis of 10 g of the powdered material using a Retsch® sieve shaker type AS200 (F. Kurt Retsch GmbH, German). The sieve shaker was fitted with eight U.S. standard sieves (Dual mfg. Co., Chicago, IL) ranging in size from 0.075 to 1.7 mm, and vibrated at a setting of 80 for 120 s. Uniformity coefficient was measured as the numerical value arrived at by dividing the width of the sieve opening that will pass 60% of the sample by the width of sieve opening that will pass 10% of the sample.

2.5. Compaction of the solid-lipid (liquisolid) powder blends

Tablets containing 130 mg of the lipid formulation were prepared by compressing the powder between the platens of a flat-faced 12 mm punches under the compaction forces stated in the experimental design (Table 3.9). Punching assembly was mounted between the platens of a Carver® press model C (Carver Inc., Wabash, IN) attached to a semiautomatic compression assembly model 2826 (Carver). Hardness of the resultant tablets were determined in triplicates using manual hardness tester (Stokes). Friability of the compacts was measured using VanKel Type™, dual chamber drum, friability tester (VanKel, Cary, NC) set at a rotation speed of 25 rpm. Five grams of tablets were allowed to rotate for 4 min (100 rotations). At the end of the run, tablets were accurately weighed and % friability was computed from the weight of tablets before and after the test.

2.6. Dissolution studies

Dissolution and release of CoQ_{10} from the solid compacts was determined using USP XXIV rotating basket apparatus (VanKel, mod. VK7000) at 37 °C. The rotating speed was 50 rpm and the dissolution medium was 900 ml of water. In this study the dissolution of CoQ_{10} was referred to as the release of CoQ_{10} lipid formulation because it is assumed that CoQ_{10} could only be dissolved in the dissolution medium when it is associated with a lipid carrier. The dissolution and characterization of CoQ_{10} lipid formulation was previously addressed by Nazzal et al. (2002b, 2002c). Dissolution studies were carried out for 12 h to evaluate the sustained release properties of the preparations. Samples (3 ml) withdrawn at fixed time intervals were filtered using a 10 μm VanKel filter and were assayed for CoQ_{10} by HPLC at 275 nm. Briefly, CoQ_{10} was analyzed using a C18, 3.9 mm × 150 mm reverse phase chromatography column (Nova-Pak; Waters, Milford, MA). The mobile phase consisted of methanol:*n*-hexane (9:1) and was pumped at a flow rate of 1.5 ml min^{-1}. The dissolution experiments were carried out in triplicates. Details of the HPLC method can be found elsewhere (Nazzal et al., 2001).

2.7. Stability studies

The optimized tablet dosage forms containing the lipid formulation were subjected to accelerated stability studies. Two ounce amber colored glass containers, each containing 45 tablets were stored at 4 °C; in temperature controlled ovens at 25 and 30 °C; in a light stability chamber at 25 °C under fluorescent light equivalent to 880-ft candle and UV irradiation (350 nm) using a 60 W black light; and in humidity chambers at 25 °C/60% RH, 30 °C/60% RH and 40 °C/75% RH. These conditions were selected to facilitate comparison of stability data without strictly adhering to the ICH guidelines which recommends 30 °C/65% RH as the intermediate storage condition. Saturated salt solutions of sodium bromide (for 60% RH) and sodium chloride (for 75% RH) were used to maintain the humidity conditions. Six tablets were removed at each time point (15 days, 1 month, 2 months and 4 months) and evaluated for their hardness and dissolution profiles.

3. Results and discussion

3.1. Response surface methodology

3.1.1. Faced-centered cubic design

Factorial designs are often used to estimate coefficients (effects) of first-order polynomial response surface (RS) models with or without interaction terms. However, in order to estimate quadratic effects, 3^n designs where n is the total number of design variables, should be used but often require an unmanageable number of design points. One of the most common second-order designs, configured to reduce the number of design points, is the central composite design. A central composite design (CCD) is a two level ($2^{(n-m)}$ or 2^n) factorial design, augmented by a replicated k_o center points and two "star" ($2n$) points positioned at $\pm\alpha$ for each factor. These $2n$ points are also called the axial points. The distance of the axial points from the origin generally varies from 1 to $\sqrt{n}$. The total number of design points is therefore

$$N = 2^{n-m} + 2n + k_o,$$

N is the number of experiments, n is the number of design variables, and m is a fraction of full factorial.

When a quadratic RS model is fit to a composite design, the factorial points contribute to estimating the linear terms and two-factor interactions. The axial points contribute to estimating the quadratic terms. Without the axial points, only the sum of the quadratic terms can be estimated. The axial points do not contribute to the estimation of interaction terms. The center points also contribute to the estimation of quadratic terms.

Face-centered cubic design (or face-centered central composite design) is obtained by setting $\alpha = 1$. This locates the star points on the centers of the faces of the cube. Spacing star points or axial points one unit from the center point brings the points lying outside the cube to lie on the boundary of the region of interest.

3.1.2. Experimental design

For the response surface methodology based on the face-centered cubic design, a total of 17 experiments were required for this study. The experimental runs and the observed responses for the 17 formulations are given in Table 3. Flowability index values, Y_7, were obtained as described previously and are given in Table 4. As seen from the table, addition of silicon dioxide and magnesium stearate improved the flow properties of the formu-

Table 3
Observed responses for the face-centered cubic design

Run	X_1	X_2	X_3	Y_1	Y_2	Y_3	Y_4	Y_5	Y_6	Y_7	Y_8
1	−1	−1	−1	16.3	38.2	81.5	83.9	86.4	3.1	80.0	0.04
2	1	−1	−1	7.1	18.3	36.3	46.7	48.5	5.0	87.0	0.04
3	−1	1	−1	21.5	53.7	84.9	85.4	90.4	3.1	77.0	0.04
4	1	1	−1	8.8	22.4	38.6	48.4	53.5	4.8	86.5	0.04
5	−1	−1	1	13.7	26.4	52.4	75.7	76.9	4.9	80.0	0.01
6	1	−1	1	10.3	21.2	35.6	44.8	45.7	6.6	87.0	0.16
7	−1	1	1	10.3	25.2	51.1	75.9	79.4	4.4	77.0	0.02
8	1	1	1	7.8	16.5	28.1	35.5	44.2	6.4	86.5	0.02
9	−1	0	0	15.6	25.0	50.6	66.9	71.6	3.8	78.0	0.04
10	1	0	0	8.6	16.1	37.5	42.5	49.2	5.9	90.0	0.06
11	0	−1	0	6.7	12.4	26.6	38.3	49.6	4.5	84.0	0.08
12	0	1	0	12.3	25.0	47.4	69.0	68.6	4.9	85.0	0.01
13	0	0	−1	4.7	21.5	28.9	37.6	40.6	3.4	87.0	0.08
14	0	0	1	13.2	16.7	29.4	39.8	42.1	4.9	87.0	0.07
15	0	0	0	6.3	11.5	25.4	38.5	49.5	4.9	87.0	0.00
16	0	0	0	9.6	12.4	28.2	37.6	54.4	4.9	87.0	0.00
17	0	0	0	6.8	12.9	23.5	35.8	50.9	4.9	87.0	0.00

lations. All preparations had a flowability index value ranging from 77 to 90, which reflects good flow in the point-score scale devised by Carr (1965). This demonstrates an improvement in the flowability of the formulations compared to a flowability index value of 61 for the immediate release formulation, which was previously optimized (Nazzal et al., 2002b) and used as the base formulation in this study. Furthermore, all preparations in the face-centered cubic design showed friability values, Y_8, less than 0.2% (Table 3). Since the differences in flowability index values and friability were insignificant among the preparations, they were not considered for the final optimization of the dosage form.

Based on the experimental design, the factor combinations resulted in solid formulations with sustained release profile of the CoQ_{10} lipid-based formulation over a time span ranging from 4 to 12 h. This can be seen in Fig. 1 that shows the dissolution profiles of the 17 formulations. Based on the preliminary dissolution data, it was of interest to examine whether a tablet dosage form could be manufactured that delivers the CoQ_{10} lipid formulation in a controlled release pattern over an 8 h time span.

The range of the response Y_5 – the cumulative percent of the CoQ_{10} self-emulsified lipid formulation released from the tablet dosage form within 8 h – were 90.4% in formulation no. 3 (maximum) and 40.6% in formulation no. 13 (minimum).

The mathematical relationships in the form of polynomial equation for the measured responses obtained with the statistical package X-STAT® are listed in Table 5. Confidence values that the regression equation would predict the observed values better than the mean for Y_1, Y_2, Y_3, Y_4, Y_5 and Y_6 were 86%, 99.9%, 99.2%, 99%, 99.8% and 100%, respectively. The polynomial equation relating the response Y_5 and the independent variables is given in Table 5. The values of X_1–X_3 were substituted in the equation to obtain the theoretical values of Y_5. The theoretical (predicted) values and the observed values were in

Table 4
Flowability index values, Y_7, for the 17 formulations evaluated in the face-centered cubic design

Run	Angle of repose		Compressibility		Angle of spatula		Uniformity coefficient		Flowability index
	°	Points	%	Points	°	Points	Units	Points	
1	39.3	18	13.1	21	44.3	18	1.74	23	80.0
2	35.3	20	8.0	23	37.5	21	1.89	23	87.0
3	39.8	17.5	15.8	19.5	46.5	17	1.74	23	77.0
4	33.8	21	8.2	23	38.8	19.5	1.89	23	86.5
5	39.3	18	13.1	21	44.3	18	1.74	23	80.0
6	35.3	20	8.0	23	37.5	21	1.89	23	87.0
7	39.8	17.5	15.8	19.5	46.5	17	1.74	23	77.0
8	33.8	21	8.2	23	38.8	19.5	1.89	23	86.5
9	40.5	17.5	15.8	19.5	44.0	18	1.91	23	78.0
10	34.3	21	5.5	25	37.5	21	1.89	23	90.0
11	35.8	18	5.3	25	40.0	18	1.68	23	84.0
12	36.5	19.5	10.5	22.5	38.5	20	1.89	23	85.0
13	36.3	19.5	5.2	25	39.5	19.5	1.57	23	87.0
14	36.3	19.5	5.2	25	39.5	19.5	1.57	23	87.0
15	36.3	19.5	5.2	25	39.5	19.5	1.57	23	87.0
16	36.3	19.5	5.2	25	39.5	19.5	1.57	23	87.0
17	36.3	19.5	5.2	25	39.5	19.5	1.57	23	87.0

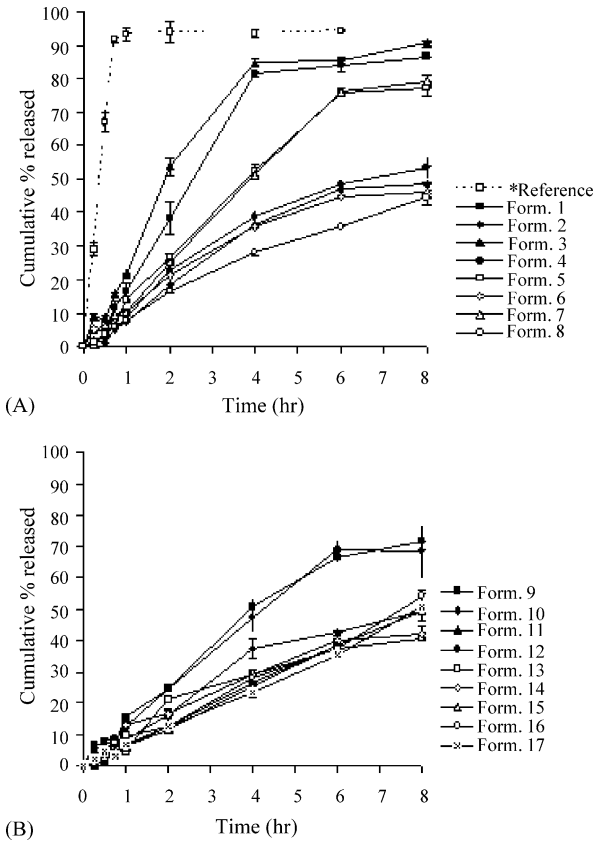

Fig. 1. Dissolution profiles of CoQ_{10} from the self-emulsified tablet formulations. (A) Reference and formulations 1–8; (B) formulations 9–17 ($n = 3$). *Reference profile refers to the tablet formulation, which was previously optimized by Nazzal et al. (2002b) to release approx. 100% of the lipid formulation within 45 min.

reasonably good agreement as seen from Table 6. The significance of the ratio of mean square variation due to regression and residual error was tested using ANOVA. The ANOVA indicated a significant ($P < 0.05$) effect of the factors on the response ($F_{cal}[12.41] > F_{crit}[7.48]$).

3.2. Effect of formulation and process variables on dissolution rate

The effect of silicon dioxide, magnesium stearate mixing time, and compression force (independent variables) on CoQ_{10} release rates (dependent variables) was demonstrated using contour and response surface plots. The effect of X_1 (amount of silicon dioxide) and X_2 (magnesium stearate mixing time) and their interaction on Y_5 (the cumulative percent of CoQ_{10} emulsified in 8 h) at a fixed level of X_3 (compression force equivalent to 1250 kg) are given in Fig. 2. At low levels of magnesium stearate mixing time, Y_5 increased from 53.5% to 85.5% when the amount of silicon dioxide decreased from 1 (5%) to −1 (1%). Similarly, at high levels of magnesium stearate mixing time, Y_5 increased from 58.6% to 92.0% when the amount of silicon dioxide decreased from 1 (5%) to −1 (1%). Due to its hydrophobicity, CoQ_{10} is strongly bound to silicon dioxide, which explains the decline in the cumulative percent of CoQ_{10} dissolved into the aqueous dissolution medium at high levels of X_1. A similar observation was made when the effect of silicon dioxide and compression force were evaluated for their effect on Y_5 at fixed level of X_2 (4 min). As seen in Fig. 3, at low levels of compression force, Y_5 increased from 40.4% to 75.2% when the amount of silicon dioxide decreased from 1 (5%) to −1 (1%). Similarly, at high levels of compression force, Y_5 increased from 36.3% to 66.9% when X_1 decreased from 1 (5%) to −1 (1%). It was reported that an increase in the amount of colloidal silicon dioxide markedly decreased the release and dissolution rate of micronized griseofulvin solid dispersion made with polyethylene glycol 3000 (Sjokvist et al., 1989). Similarly, incomplete recovery of griseofulvin in the dissolution medium was observed when the drug was mixed with high levels of silicon dioxide (Abdallah et al., 1983).

Table 5
Regression equations for the responses[a]

$$Y_1 = 8.35 - 3.48X_1 + 0.65X_2 + 1.99X_1X_3 - 1.59X_2X_3 + 3.17X_1^2 + 0.57X_2^2$$
$$Y_2 = 13.62 - 7.39X_1 + 2.62X_2 - 4.80X_3 - 1.86X_1X_2 + 4.66X_1X_3 - 3.18X_2X_3 + 5.89X_1^2 + 4.04X_2^2 + 4.43X_3^2$$
$$Y_3 = 27.47 - 14.46X_1 + 1.76X_2 - 7.36X_3 + 6.45X_1X_3 + 15.29X_1^2 + 8.22X_2^2$$
$$Y_4 = 39.64 - 16.99X_1 + 2.48X_2 - 3.03X_3 - 1.17X_1X_2 - 1.53X_2X_3 + 13.29X_1^2 + 12.26X_2^2 - 2.69X_3^2$$
$$Y_5 = 49.78 - 16.36X_1 + 2.90X_2 - 3.11X_3 - 0.37X_1X_2 + 1.06X_1X_3 - 1.02X_2X_3 + 11.98X_1^2 + 10.63X_2^2 - 7.10X_3^2$$
$$Y_6 = 4.67 + 0.94X_1 + 0.78X_3 + 0.29X_1^2 + 0.17X_2^2 - 0.39X_3^2$$

[a] The terms with small coefficients (less than 0.005) were deleted from the equation.

Table 6
Observed and predicted values of the response Y_5

Run	Observed	Predicted	Residuals (observed − predicted)
1	86.41	81.53	4.88
2	48.49	47.46	1.03
3	90.43	90.11	0.32
4	53.53	54.54	−1.01
5	76.92	75.23	1.69
6	45.73	45.38	0.35
7	79.39	79.75	−0.36
8	44.20	48.40	−4.20
9	71.60	78.12	−6.52
10	49.23	45.41	3.82
11	49.57	57.52	−7.95
12	68.56	63.32	5.24
13	40.57	45.79	−5.22
14	42.09	39.57	2.52
15	49.48	49.78	−0.30
16	54.38	49.78	4.60
17	50.90	49.78	1.12

Source	df	SS	MS	*F*-ratio
ANOVA for Y_5				
Total (corrected)	16	4249		
Regression[a]	9	3999	444.3	
Residual	7	250	35.8	12.41

[a] Confidence that the regression equation predicts the observed values better than the mean = 99.8%.

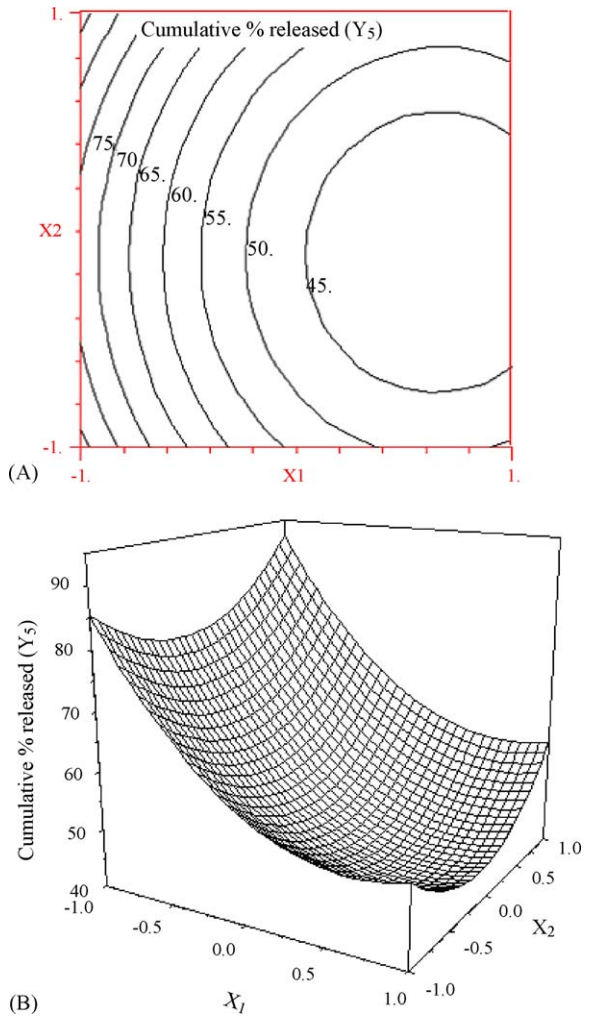

Fig. 2. (A) Contour plot and (B) response surface plot (3D) showing the effect of the amount of silicon dioxide (X_1) and magnesium stearate mixing time (X_2) on the response Y_5 (cumulative percent of CoQ_{10} released in 8 h).

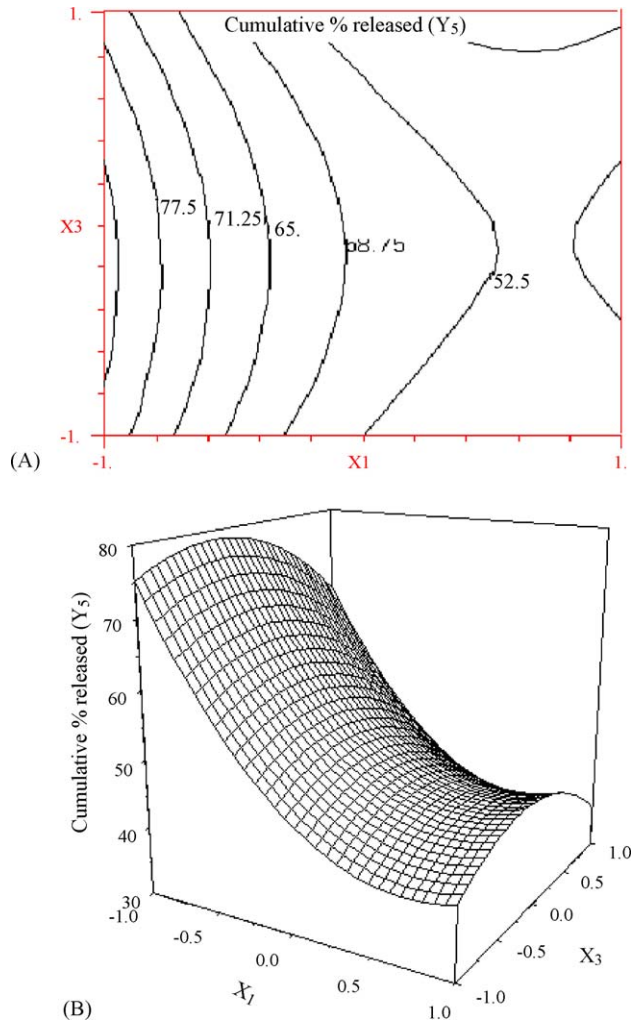

Fig. 3. (A) Contour plot and (B) response surface plot (3D) showing the effect of the amount of silicon dioxide (X_1) and compression force (X_3) on the response Y_5 (cumulative percent of CoQ_{10} released in 8 h).

In the aqueous dissolution medium, a tablet dosage form of a lipid formulation undergoes slow surface erosion. The rate of dissolution and degree of surface erosion are primarily dependent on the amount of silicon dioxide added to the formulation and the applied compression force. Moistened silicates retard tablet disintegration by inhibiting moisture migration. Tight bonding between particles by the applied force further inhibits moisture penetration and delays exposure of the lipid formulation to the dissolution medium. As seen in Fig. 3, at high levels of silicon dioxide, Y_5 decreased from 40.4% to 36.3% as the applied force increased from −1 (500 kg) to 1 (3000 kg). Similarly, at low levels of silicon dioxide, Y_5 decreased from 75.2% to 66.9% as the applied force increased from −1 to 1. The effect of compression force on dissolution rate can be demonstrated with the help of Fig. 4 showing the effect of X_3 (compression force) and X_2 (magnesium stearate mixing time) and their interaction on Y_5 at fixed levels of silicon dioxide (3%). At low levels of X_2, Y_5 decreased from 52.5% to 48.3% as compression force increased from −1 (500 kg) to 1 (3000 kg). Similarly, at high levels of X_2, Y_5 decreased from 60.3% to 52.1% as compression force increased from −1 to 1. Increase in compression force was shown to decrease the dissolution rate of phenobarbital tablets (Rehula et al., 1985) and griseofulvin solid dispersion made by co-melt with xylitol (Sjokvist and Nystrom, 1991).

Magnesium stearate mixing time (X_2) had a moderate effect on the dissolution rate of the formulations. Increasing the mixing time increased the cumulative percent of lipid formulation emulsified in 8 h. As seen in Fig. 4, at low levels of compression force (X_3), Y_5 increased from 52.5% to 60.3% as magnesium stearate mixing time increased from −1 (2 min) to 1 (6 min). Similarly, at high levels of X_3, Y_5 increased from 48.3% to 52.1% as magnesium stearate mixing time increased from −1 to 1. Similar observation can be seen from Fig. 2. At low levels of silicon dioxide, Y_5 increased from 85.5% to 92.0% as magnesium stearate mixing time increased from −1 to 1. Similarly, at high levels of silicon dioxide, Y_5 increased from 53.5% to 58.6% as magnesium stearate mixing time increased from −1 to 1. A possible explanation for this behavior is that colloidal silica interacts with the free fraction of magnesium stearate resulting in spherical agglomerates (Johansson and Nicklasson,

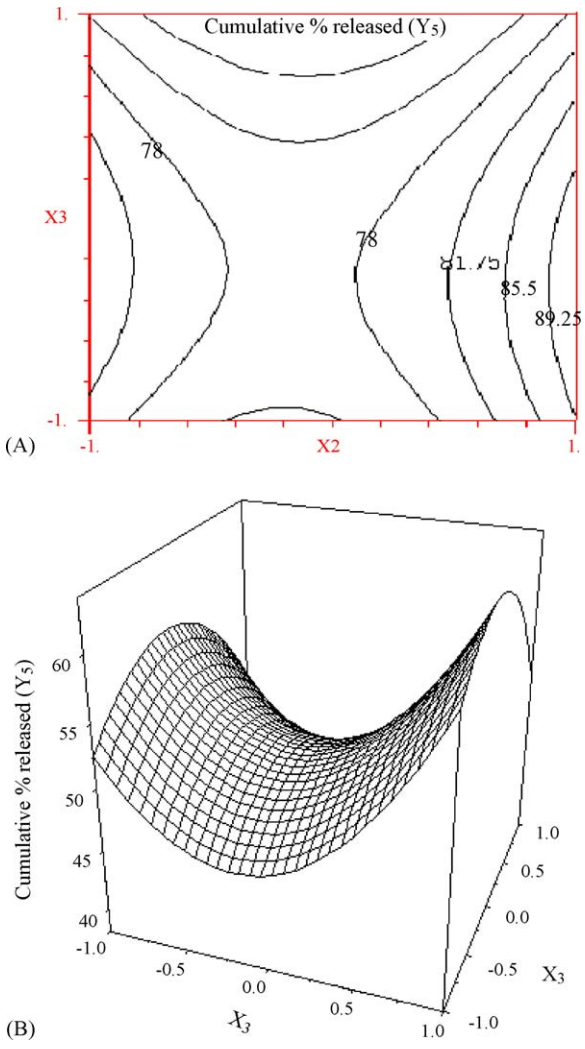

Fig. 4. (A) Contour plot and (B) response surface plot (3D) showing the effect of the magnesium stearate mixing time (X_2) and compression force (X_3) on the response Y_5 (cumulative percent of CoQ_{10} released in 8 h).

1986). As a consequence, the inhibitory effect of the individual ingredients on the dissolution rate is reduced. The interaction between magnesium stearate and colloidal silicon dioxide during the mixing process was studied by Lerk and Bolhuis (1977) using electron micrographs and X-ray maps. This interaction is further promoted by the mixing time, hence increased dissolution rate of the lipid formulation from the tablet dosage form.

3.3. Optimization of the formulation and process parameters

After generating the polynomial equations relating the dependent and independent variables, the process was optimized for the response Y_5. Optimization was performed to obtain the levels of X_1–X_3, which maximize Y_5 at constrained conditions of Y_1 through Y_6. Constraints were made in an effort to obtain an optimized sustained release tabled dosage form that delivers the CoQ_{10} self-nanoemulsified formulation over 8 h following a zero-order release kinetics. This was achieved by having constraints on the release rate so that 12.5% of the formulation is released from the tablet per hour. The optimized levels of the process variables that achieve the desired dissolution profile and their predicted Y_1–Y_6 responses are given in Table 7. To verify these values, a new formulation was prepared according to the predicted levels of X_1, X_2 and X_3. A representative dissolution profile of the optimized formulation is given in Fig. 5. Experimentally derived Y_5 values were in a close agreement with the predicted values. The predicted and observed values are shown in Table 7. These results demonstrate the reliability of the optimization procedure in predicting the effect of process variables on the dissolution behavior of the "liquisolids" or solid dosage forms of lipid self-emulsified drug delivery systems.

Table 7
Optimized values obtained by the constraints applied on Y_1–Y_6

Variable	Nominal values	Response	Expected values	Observed values
X_1	1.06%	Y_1	13.9	13.6
X_2	2 min	Y_2	23.9	26.2
X_3	1670 kg	Y_3	55.0	54.7
		Y_4	75.4	77.2
		Y_5	80.4	87.2
		Y_6	4.6	4.8

3.4. Stability studies

Hardness and dissolution profiles of the optimized sustained release tablets containing the CoQ_{10} self-emulsified formulation were evaluated at temperature, light, and humidity conditions specified in the experimental section. Hardness of the tablets subjected to different stability conditions are given in Table 8.

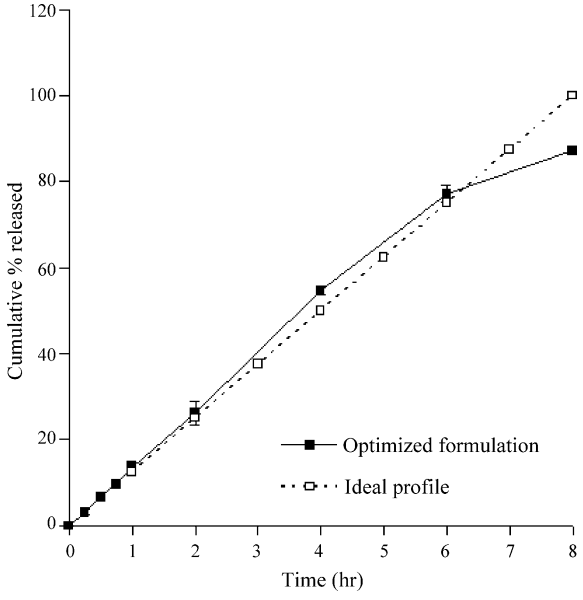

Fig. 5. Dissolution profiles of the optimized sustained-release CoQ_{10} self-emulsified tablet dosage form ($n = 3$) and the ideal 8-h zero-order release profile.

Table 8
Hardness (kgf)[a] of the CoQ_{10} sustained-release SEDDS tablet formulation stored at different stability conditions

Time	4 °C	25 °C	25 °C/60%	25 °C (light)	30 °C	30 °C/60%	40 °C/75%
Initial	5.0 ± 0.4	5.0 ± 0.4	5.0 ± 0.4	5.0 ± 0.4	5.0 ± 0.4	5.0 ± 0.4	5.0 ± 0.4
15 days	4.5 ± 0.2	5.0 ± 0.4	5.0 ± 0.4	5.0 ± 0.4	4.5 ± 0.2	5.0 ± 0.4	3.5 ± 0.4
1 month	5.5 ± 0.6	5.0 ± 0.4	5.0 ± 0.4	4.5 ± 0.2	4.5 ± 0.2	4.5 ± 0.2	3.5 ± 0.4
2 months	5.0 ± 0.4	5.0 ± 0.4	5.0 ± 0.4	4.5 ± 0.2	5.0 ± 0.4	5.0 ± 0.4	3.0 ± 0.4
4 months	5.0 ± 0.4	5.0 ± 0.4	5.0 ± 0.4	4.5 ± 0.2	3.5 ± 0.4	3.5 ± 0.4	2.5 ± 0.4

[a] kgf: kilogram-force.

The dissolution profiles of the CoQ_{10} SNEDDS formulation at different stability conditions are given in Figs. 6 and 7. Dissolution profiles were compared with a model independent approach using a difference factor (f_1) and a similarity factor (f_2) (Moore and Flanner, 1996). Although the f_1 and f_2 tests were developed for a larger sample size, their application in this study, where $n = 3$, was intended to be instructive but not definitive.

The difference factor (f_1) calculates the percent difference between the reference and a test formulation at each time point and is a measurement of the relative error between the two

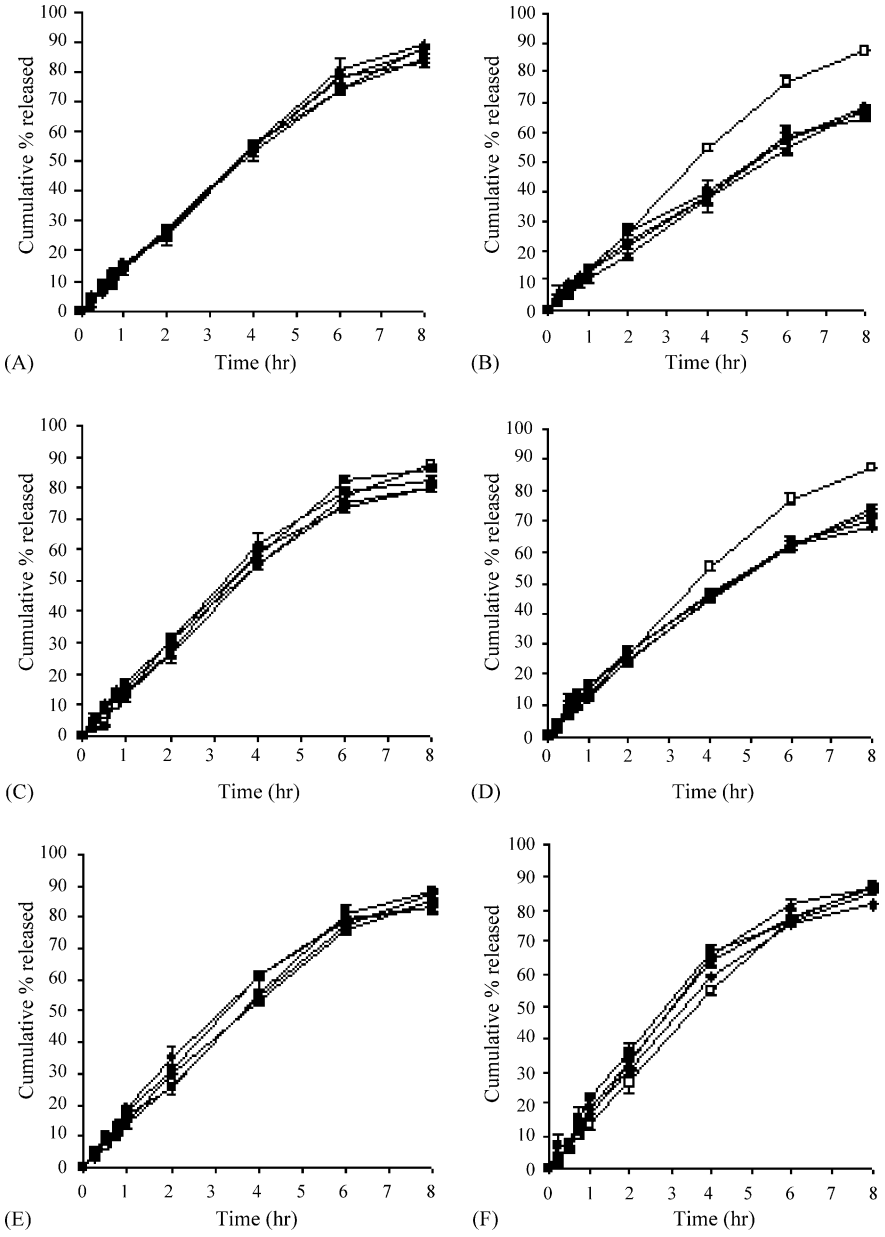

Fig. 6. Dissolution profiles of the CoQ_{10} sustained-release self-emulsified tablet formulations ($n = 3$) when stored at (A) 4 °C, (B) 25 °C, (C) 25 °C/60% RH, (D) 30 °C, (E) 30 °C/60% RH, and (F) 40 °C/75% RH [□, time zero; ■, 15 days; ♦, 1 month; ▲, 2 months; ●, 4 months].

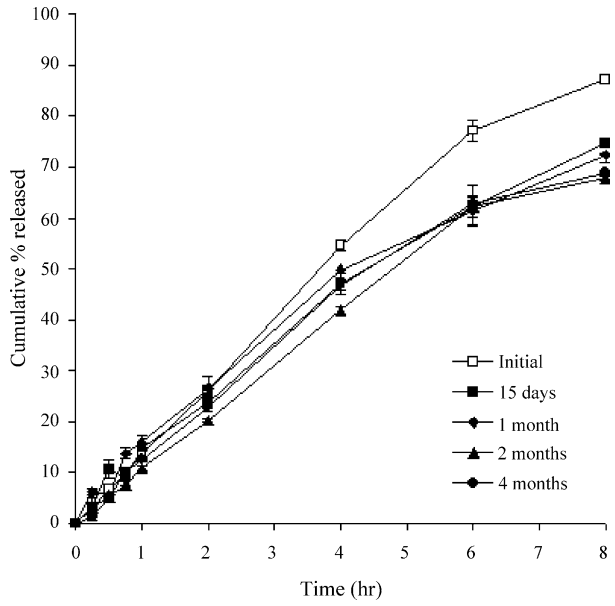

Fig. 7. Dissolution profiles of the CoQ_{10} sustained-release self-emulsified tablet formulation stored in the light stability chamber at 25 °C ($n = 3$).

curves:

$$f_1 = \frac{\sum_{t=1}^{n} |R_t - T_t|}{\sum R_t} \times 100$$

where R_t is the cumulative percent drug dissolved for the reference sample at time t, T_t the cumulative percent drug dissolved for the test sample at time t, and n is the number of time points.

The similarity factor (f_2) is a logarithmic reciprocal square root transformation of the sum of squared error and is a measurement of the similarity in the percent dissolution between the two curves:

$$f_2 = 50 \log \left\{ \left[1 + \frac{1}{n} \sum_{t=1}^{n} W_t (R_t - T_t)^2 \right]^{-0.5} \times 100 \right\}$$

where W_t is an optional weight factor. W_t is applied to the value or values that are deemed more important than others. It was taken as one since all the dissolution time points were treated equally.

The dissolution profile of fresh tablets was considered as reference profile whereas the dissolution profiles of the tablets collected periodically during the stability studies were considered as test profiles. For curves to be considered similar, f_1 values should be close to 0, and f_2 values should be close to 100. Generally, f_1 values up to 15 (0–15) and f_2 values greater than 50 (50–100) ensure similarity or equivalence of the two curves (CDER, 1997). The f_1 and f_2 fit factors for the CoQ_{10} sustained-release SNEDDS formulation stored at different stability conditions are given in Table 9.

The rate and extent of SNEDDS release from the tablets stored at 4 °C and the hardness of the compacts was similar to that of the reference formulation. The extent of CoQ_{10} solubilized into the dissolution medium, however, decreased for the samples stored at 25 °C, 25 °C in light stability chamber, or 30 °C. This can be seen by the high f_1 values (>15) and low f_2 values (<50), which are given in Table 9. The similarity of the dissolution profile for the sample stored at 25 °C and those kept in a light stability chamber, and the absence of light degradation peaks in the HPLC chromatographs, suggest that the solid state stability of CoQ_{10} was maintained in the amber vials that were used to store the tablets. The hardness of these preparations did not change with time except for the tablets stored at 30 °C for 4 months (Table 8). This was also observed for the tablets stored at 30 °C/60% RH. A decrease in hardness at higher temperatures might be due to a partial leakage of the formulation into the backing support of the tablets.

At higher humidity, however, no change was observed in the dissolution profile for samples stored at 25 °C/60% RH and 30 °C/60% RH when compared to the reference profile. The effect of humidity on the rate and extent of dissolution is not fully understood. It is probable that the vapor pressure within the vials prevented the separation of the lipid formulation. At low relative humidity and low vapor pressure, lemon oil phases out of the lipid formulation and adsorbs onto the colloidal silicates or the supporting MCC layer, hence reducing the efficiency of the eutectic formulation to melt and emulsify into the dissolution medium.

The melting and leakage of the lipid formulation to the surface of the tablets stored at 40 °C/75% RH was visually evident and explains the initial burst effect and the higher release rates

Table 9
f_1 and f_2 values for the CoQ_{10} sustained-release SEDDS tablet formulation stored at different stability conditions

Time	4 °C	25 °C	25 °C/60% RH	25 °C (light)	30 °C	30 °C/60% RH	40 °C/75% RH
f_1							
Initial	0.0	0.0	0.0	0.0	0.0	0.0	0.0
15 days	5.3	24.3	8.0	18.2	19.2	7.4	16.3
1 month	5.3	24.5	11.7	16.4	22.7	6.2	9.2
2 months	6.5	28.0	10.1	22.1	16.6	11.6	11.2
4 months	7.2	21.7	10.2	17.4	17.2	13.3	10.9
f_2							
Initial	100.0	100.0	100.0	100.0	100.0	100.0	100.0
15 days	81.3	47.2	74.4	55.9	53.7	74.8	59.1
1 month	81.1	47.8	68.0	55.8	51.2	78.6	72.7
2 months	78.2	45.7	69.4	50.9	55.2	68.9	65.5
4 months	76.5	48.6	70.2	53.9	55.2	65.1	66.6

at the initial time points. Formulation leakage onto the backing support layer of the tablets explains the decline in the hardness with time (Table 8). The extent of dissolution for the samples stored at 40 °C/75% RH, however, was comparable to that of the reference formulation suggesting stability of the lipid formulation against degradation at high heat and humidity. No weight gain was observed for all the samples examined throughout the stability study.

4. Conclusions

Common processing parameters such as those evaluated in this study – amount of colloidal silicon dioxide (X_1), magnesium stearate mixing time (X_2), and compression force (X_3) – have a profound effect on the release of lipid formulations from their solid carriers. In this study, the quantitative effect of these factors at different levels was estimated by response surface methodology and was predicted and expressed in polynomial equations. Silicone dioxide had a particularly significant effect on lipid release. While silicates are common adjuvants, their effect should be investigated when manufacturing lipid-solid compacts. Due to their unique and strong interaction with lipids, silicates have an effect on both the rate and extent of lipid release from its solid carrier. Observed responses, however, might be attributed to the nature of the eutectic SEDDS formulation which was incorporated into the tablet dosage form. The emulsification of this formulation relies on the eutectic interaction between CoQ_{10} and the lipid excipients. Adsorption of lemon oil on both the silicates and magnesium stearate, and the compression mediated diffusion of the lipid within the solid matrix could be considered as the primary factors responsible for the delayed release effect. This study, however, demonstrated that a tablet dosage form could be manufactured to release a lipid formulation in a controlled release pattern without the need for complicated manufacturing techniques. To further verify the utility of statistical optimization techniques, response surface methodology was used to predict the levels of the factors X_1, X_2, and X_3 required to obtain an optimum formulation with a zero-order lipid release pattern. A new formulation, which was prepared according to these levels, was in close agreement with the predicted values. While the optimized formulation was stable at lower storage temperatures, special attention should be made to the effect of high temperature and humidity conditions on the release of lipids from these dosage forms. It was evident from the reported data that higher temperatures could have a devastating effect on the physical stability of the preparations. Unfortunately, while many studies report novel solid-lipid compacts, very few have discussed the impact of storage conditions on the physical properties of these compacts.

References

Abdallah, H.Y., Khalafallah, N., Khalil, S.A., 1983. Influence of dispersion method on particle size and dissolution of griseofulvin silicon dioxide triturations. Drug Dev. Ind. Pharm. 9, 795–808.

Alderborn, G., Nystrom, C., 1982. Studies on direct compression of tablets. Part 4. Effect of particle size on the mechanical strength of tablets. Acta Pharm. Suec. 19, 381–390.

Cannon, J.B., 2005. Oral solid dosage forms of lipid-based drug delivery systems. Am. Pharmaceut. Rev. 8, 108–115.

Carr, R.L., 1965. Evaluating flow properties of solids. Chem. Eng. 18, 163–168.

Center for Drug Evaluation and Research (CDER), 1997. Guidance for Industry: Dissolution Testing of Immediate Release Solid Oral Dosage Forms. Food and Drug Administration, Rockville, MD.

Charman, S.A., Charman, W.N., Rogge, M.C., Wilson, T.D., Dukto, F.J., Pouton, C.W., 1992. Self-emulsifying drug delivery systems: formulation and biopharmaceutic evaluation of an investigational lipophilic compound. Pharmaceut. Res. 9, 87–93.

Craig, D.Q.M., Lievens, H.S.R., Pitt, K.G., Storey, D.E., 1993. An investigation into the physico-chemical properties of self-emulsifying systems using low frequency dielectric spectroscopy, surface tension measurements and particle size analysis. Int. J. Pharm. 96, 147–155.

Dabbagh, M.A., Ford, J.L., Rubinstein, M.H., Hogan, J.E., 1996. Effects of polymer particle size, compaction pressure and hydrophilic polymers on drug release from matrices containing ethylcellulose. Int. J. Pharm. 140, 85–95.

Dong, L., Shafi, K., Wong, P., Wan, J., 2002. L-Oros® Sofcap™ for controlled release of non-aqueous liquid formulations. Drug Deliv. Technol. 2, 52–55.

Duberg, M., Nystrom, C., 1986. Studies on direct compression of tablets XVII. Porosity–pressure curves for the characterization of volume reduction mechanisms in powder compression. Powder Technol. 46, 67–75.

Gao, Z.G., Choi, H.G., Shin, H.J., Park, K.M., Lim, S.J., Hwang, K.J., Kim, C.K., 1998. Physicochemical characterization and evaluation of a microemulsion system for oral delivery of cyclosporine A. Int. J. Pharm. 161, 75–86.

Hariharan, M., Wheatley, T.A., Price, J.C., 1997. Controlled-release tablet matrices from carrageenans: compression and dissolution studies. Pharm. Dev. Technol. 2, 383–393.

Jannin, V., Chambin, O., 2005. Self emulsifying drug delivery systems. STP Pharma Pratiques 15, 247–254.

Johansson, M.E., Nicklasson, M., 1986. Investigation of the film formation of magnesium stearate by applying a flow through dissolution technique. J. Pharm. Pharmacol. 38, 51–54.

Khan, K.A., Musikabhumma, P., Rubinstein, M.H., 1983. Effect of mixing time of magnesium stearate on the tableting properties of dried microcrystalline cellulose. Pharm. Acta Helv. 58, 109–111.

Kim, C., Shin, H., Yang, S., Kim, J., Oh, Y., 2001. Once-a-day oral dosing regimen of cyclosporine A: combined therapy of cyclosporine A premicroemulsion concentrates and enteric coated solid-state premicroemulsion concentrates. Pharmaceut. Res. 18, 454–459.

Lerk, C.F., Bolhuis, G.K., 1977. Interaction of lubricants and colloidal silica during mixing with excipients. 2. Its effect on wettability and dissolution velocity. Pharm. Acta Helv. 52, 39–44.

Liao, C., Jarowski, C.I., 1984. Dissolution rates of corticoid solutions dispersed on silicas. J. Pharm. Sci. 73, 401–403.

Moore, J.W., Flanner, H.H., 1996. Mathematical comparison of dissolution profiles. Pharm. Technol. 20, 64–74.

Morasso, M.I., Salas, J., Arancibia, A., 1988. Effect of mixing on the biopharmaceutical properties of sulfadiazine tablets. Farmaco Ed. Prat. 43, 177–188.

Murray, J., 1994. X-Stat, Version 2.02®, Statistical Experiment Design, Data Analysis and Nonlinear Optimization. Wiley, New York.

Nazzal, S., Khan, M.A., 2002. Response surface methodology for the optimization of ubiquinone self-emulsified drug delivery system. AAPS PharmSciTech. 3 (article 3).

Nazzal, S., Guven, N., Reddy, I.K., Khan, M.A., 2002a. Preparation and characterization of CoQ_{10}—Eudragit® solid dispersion. Drug Dev. Ind. Pharm. 28, 49–57.

Nazzal, S., Nutan, M., Palamakula, A., Shah, R., Zaghloul, A.A., Khan, M.A., 2002b. Optimization of a self-nanoemulsified tablet dosage form of ubiquinone using response surface methodology: effect of formulation ingredients. Int. J. Pharm. 240, 103–114.

Nazzal, S., Smalyukh, I.I., Lavrentovich, O.D., Khan, M.A., 2002c. Preparation and in-vitro characterization of a eutectic based semisolid self-

nanoemulsified drug delivery system (SNEDDS) of ubiquinone: mechanism and progress of emulsion formation. Int. J. Pharm. 235, 247–265.

Nazzal, S., Zaghloul, A.A., Khan, M.A., 2002d. Effect of extra-granular microcrystalline cellulose on compaction, surface roughness and in-vitro dissolution of a self-nanoemulsified solid dosage form of ubiquinone. Pharmaceut. Technol. 26, 86–98.

Nazzal, S., Zaghloul, A.A., Reddy, I.K., Khan, M.A., 2001. Analysis of ubidecarenone (CoQ_{10}) aqueous samples using reversed phase liquid chromatography. Die Pharm. 56, 394–396.

Newton, R.M., Petterson, J., Podczeck, F., Clarke, A., Booth, S., 2001. The influence of formulation variables on the properties of pellets containing a self-emulsifying mixture. J. Pharm. Sci. 90, 987–995.

Perng, C.H., Kearney, A.S., Patel, K., Palepu, N.R., Zuber, G., 1998. Investigation of formulation approaches to improve the dissolution of SB-210661, a poorly water soluble 5-lipoxygenase inhibitor. Int. J. Pharm. 176, 31–38.

Pouton, C.W., 2000. Lipid formulations for oral administration of drugs: non-emulsifying, self-emulsifying and 'self-microemulsifying' drug delivery systems. Eur. J. Pharm. Sci., S93–S98.

Rehula, A., Rehulova, M., Muzik, M., 1985. Effect of changes in compression pressure on dissolution of drugs from tablets. Folia Pharm. 8, 35–42.

Sjokvist, E., Nystrom, C., 1991. Physicochemical aspects of drug release. Part 11. Tableting properties of solid dispersions, using xylitol as carrier material. Int. J. Pharm. 67, 139–153.

Sjokvist, E., Nystrom, C., Alden, M., 1989. Physicochemical aspects of drug release. Part 9. Investigation of some factors that impair dissolution of drugs from solid particulate dispersion systems. Int. J. Pharm. 54, 161–170.

Spireas, S.S., Jarowski, C.I., Rohera, B.D., 1992. Powdered solution technology: principles and mechanism. Pharm. Res. 9, 1351–1358.

Spireas, S., Sadu, S., 1998. Enhancement of prednisolone dissolution properties using liquisolid compacts. Int. J. Pharm. 166, 177–188.

Sun, C., Grant, D.J.W., 2001. Effect of initial particle size on the tableting properties of L-lysine monohydrochloride dihydrate powder. Int. J. Pharm. 215, 221–228.

Takashima, Y., Yuasa, H., Kanaya, Y., Nomura, I., Shinozawa, K., 1999. Reduction of tablet coloration at tableting for oily medicine (tocopheryl nicotinate). Int. J. Pharm. 187, 125–135.

Wang, L.H., Chowhan, Z.T., 1990. Drug-excipient interactions resulting from powder mixing. Part 5. Role of sodium lauryl sulfate. Int. J. Pharm. 60, 61–78.

Yang, K.Y., Glemza, R., Jarowski, C.I., 1979. Effect of amorphous silicon dioxide on drug dissolution. J. Pharm. Sci. 68, 560–565.